ARTICLE

Effect of Polymerisation by Microwave on the Physical Properties of Molecularly Imprinted Polymers (MIPs) Specific for Caffeine

Received 00th January 20xx,
Accepted 00th January 20xx

DOI: 10.1039/x0xx00000x

Heli A. Brahmbhatt,[a] Alexander Surtees[b], Cavan Tierney[c], Oluwabujunmi A. Ige[c], Elena V. Piletska[d], Thomas Swift[b] and Nicholas W. Turner[a,c*]

Molecularly Imprinted Polymers (MIPs) are a class of polymeric materials that exhibit highly specific recognition properties towards a chosen target. These "smart materials" offer robustness to work in extreme environmental conditions and cost effectiveness; and have shown themselves capable of the affinities/specificities observed of their biomolecular counterparts. Despite this, in many MIP systems heterogeneity generated in the polymerisation process is known to affect the performance. Microwave reactors have been extensively studied in organic chemistry because they can afford fast and well-controlled reactions, and have been used for polymerisation reactions; however, their use for creating MIPs is limited. Here we report a case study of a model MIP system imprinted for caffeine, using microwave initiation. Experimental parameters such as polymerisation time, temperature and applied microwave power have been investigated and compared with polymers prepared by oven and UV irradiation. MIPs have been characterised by BET, SEM, DSC, TGA, NMR, and HPLC for their physical properties and analyte recognition performance. The results suggest that the performance of these polymers correlates to their physical characteristics. These characteristics were significantly influenced by changes in the experimental polymerisation parameters, and the complexity of the component mixture. A series of trends were observed as each parameter was altered, suggesting that the performance of a generated polymer could be possible to predict. As expected, component selection is shown to be a major factor in the success of an imprint using this method, but this also have significant effect on the quality of resultant polymers suggesting that only certain types of MIPs can be made using microwave irradiation. This work also indicates that the controlled polymerisation conditions offered by microwave reactors could open a promising future in the development of MIPs with more predictable analyte recognition performance, assuming material selection loans itself to this type of initiation.

Introduction

Molecularly Imprinted Polymers (MIPs) are a class of polymeric materials that exhibit highly specific recognition properties towards a chosen target. These "smart materials" offer a cost-effective route to prepare materials with a robust capability to work in extreme environmental conditions, and have shown themselves capable of the affinities/specificities observed of their biomolecular counterparts. [1] The attractiveness of this technique lies in the sheer flexibility of the technique allowing materials based on the same principle to be created as bulk materials, surfaces, supported particles or nanomaterials. [2,3] By far the most common of these are those polymers, made into bulk monoliths, and ground down in particulates of sieved size for use in solid phase extraction, or solution depletion studies. Often this method is used as a proof-of-principle to show an imprint has been created before further, more complex studies follow.

Commonly MIP monoliths are obtained by thermal initiation of azo compounds leading to free radical polymerisation. This is often performed in an oven or an immersive bath. Despite the ease of preparation, this type of heating results in poor control over the polymerisation kinetics and induces poor batch-to-batch variability and increased heterogeneity in the resultant polymeric materials. [1] A typical reaction can take up to 24 hours. Heating of material via an external source, such as an oven, or oil-/sand bath occurs via conduction, which means the heat distribution depends on the thickness and thermal conductivity of the reaction vessel. Moreover, the heat distribution within the material is driven by convection, which is largely affected by its volumes as well, and this alters as a reaction progresses as the materials changes phase.[4] This led to an imbalance in how the reaction is heated - polymer material near the vessel wall will be heated differently to that in the middle of the reaction solution.

With poor control over the internal polymerisation temperatures, exothermic reactions such as free radical polymerisations can result into excessive internal energy when being held in an oven. This leads to auto-acceleration which results into inconsistent and uncontrolled heating. For example the Piletsky group showed that while the "heating temperature" maybe set at 60 °C the core of the reaction can reach ~130 °C.[5] This will have detrimental effects on the make-up of resulting polymers; especially if it is a MIP, as the initial formation of stable monomer-template complexes in the pre-

[a] School of Life, Health and Chemical Sciences, The Open University, Milton Keynes, Buckinghamshire, MK7 6AA, UK.
[b] Department of Chemistry and Biosciences, University of Bradford, Bradford, BD7 1DP, UK
[c] Department of Chemistry, University of Leicester, Leicester, LE1 7RH, UK
[d] School of Pharmacy, De Montfort University, Leicester, LE2 7BY, UK
Electronic Supplementary Information (ESI) available: Additional thermal characterisation (DSC/TGA) details. See DOI: 10.1039/x0xx00000x

polymerisation mixture, which are formed by comparatively weaker non-covalent interactions, are required to remain if an imprint is to be successful. Therefore, elevated energy of the pre-polymerisation mixture can adversely affect formation of stable monomer-template assemblies, which are very crucial for the formation of template specific binding sites within the polymers.[6] Different conditions will lead to different chain versus step reactions in a polymerisation which in turn will lead to differences in the internal structure of the resulting polymer. Hence, traditionally prepared polymers are likely to have non-homogenous make-up in their internal structure as well as their macromolecular structure such as, porosity and surface area. This can eventually affect their template recognition performance. [5]

On the other hand, UV polymerisation by lamp or focussed beam is faster compared to its thermal counterparts such as those carried out by an oven or oil-bath (~2-6 hrs depending on vessel, reaction components and light source intensity). UV polymers tend to be more homogenous and have improved performance, however some studies suggest that UV polymers show lower surface area and lower porosity which can be detrimental to their performance. [7]

Alongside thermal and UV synthetic methods, a third option, namely microwave irradiation (MWI) could be a potential attractive alternative. MWI has been used in synthetic chemistry for the past 40 years with extremely quick and controlled reactions observed, while still maintaining excellent homogeneity, when compared to the conventional heating sources[4]. Over the same period, a significant body of research has developed exploring the use of MWI with polymerisation reactions. One common finding in most of these studies is that microwave (MW) reactors significantly enhance the rate of the monomer conversion in comparison to its traditional counterparts. This means that MWI can significantly enhance polymerisation kinetics without affecting the monomer conversion that is usually achieved with traditional methods. Faster polymerisations could be beneficial to imprinting as it could ease the scale-up issues for industrial scale preparation of the MIPs, so long as the resultant polymers have comparable physical properties and performance. It is important to point out that a lot of work in this area focuses one studies on single component systems. MIPs tend to have several components, commonly at least one functionalised monomer and a separate cross-linker which add to the complexity of the reaction.

Where traditional heating parameters have been studied well in detail, the MWI has not been investigated thoroughly for the MIP preparation. Only a few studies have been reported some two decades ago where MW heating was found to enhance the polymerisations significantly, not to mention this study were also based on non-imprinted polymers.[8] [9] Both these studies found that faster MW heating significantly improved polymerisation kinetics. At the same time, different MW heating rates showed considerable differences between their polymerisation kinetics. This suggested that different heating rates could play a crucial role in defining the properties of the MIPs, given the susceptibility of the pre-polymerisation complexation to thermodynamic changes. Hence, there is a strong need to understand as to how the variables associated with MW and traditional heating can the polymerisation process as well as the quality of the MIPs, if this is to be used as an alternative source of energy.

The use of MWI has been reported in the MIP literature mainly as a method for the template removal. MW assisted template removal is gaining interest in the areas of MIP preparation as it avoids using large quantities of the solvents unlike Soxhlet extraction. [10] [11] [12] However, only a handful of studies have explored the real scope of MW assisted MIP preparation.

One of the first attempts were made by Turner who reported caffeine imprinted MIP monoliths cured by MWI (150 W for 15 minutes).[13] For the first time, a direct comparison of MWI and oven polymerisations was made by comparing the physicochemical properties of their MIPs. This study also highlighted that the performance of the MIPs was greatly influenced by their physical properties, such as surface area, pore volume, degree of cross-linking and morphology. Although the MWI MIPs showed slightly lower template binding capacity, their imprinting efficiency was comparatively higher than thermal MIPs made in the oven. Since the imprinting efficiency of the MIPs is the measure of their selective binding sites, controlled MWI polymerisation might result into more stable monomer-template assemblies. MWI significantly enhanced polymerisation kinetics here as well, with polymerisation achieved in just fifteen minutes against 24 hours in the oven.

Around the same time Saifuddun used MW irradiation (applying 200 W irradiation power) for five minutes to polymerise α-tocotrienol imprinted polyacrylamide on the surface of microspheres.[14] The polymerisation kinetics achieved with the MW reactor were significantly faster and they also showed improved template recognition. The same group presented another study where they analysed physical properties of the MWI MIPs. From the correlation analysis between the morphology and the performance, they found that the MW MIPs exhibited rougher surface with higher pore volume and performed better than that of their corresponding NIP. MW irradiation showed faster and improved grafting of the acrylamide MIP on the chitosan microbeads. However, this study lacked a direct comparison between the MWI with the traditional heating. [15]

Another study reported preparation of the MIP magnetic microbeads by precipitation in a MW reactor. The MIPs were characterised for their physical properties and template binding performance. Thermogravimetric analysis of the MIPs showed their considerably good stability. The MWI MIPs also resulted into more homogenous particle morphology, shape and narrow particle size distribution in comparison to conventional UV polymerisation. The study was extended to template binding experiments where MIPs showed selectivity and specificity towards the target template. The entire preparation of MW MIP magnetic microbeads took less than an hour compared to 14-24 hours long by traditional means. [16,17] Further studies by Hou [18] , Kueseng [19], Schwarz [20], Jin [21], Chen [22], Seifi [23] and Xu [12] all supported the studies above in that polymers made by MWI exhibit different properties than oven counterparts.

These studies correlated the physical properties of the MIPs to their recognition performance, it did not explore different experimental parameters and their effect in the properties of the MIPs. This is a common thread seen in the literature. Despite a significant number of imprinting studies (~1100 papers in 2018) only a few papers [24] [5,25,26] focus on the physical properties and effects of polymerisation conditions – most studies focus on the application. Simply put, if the polymer performs as expected, studies on the polymers physical properties are often not carried out. Experimental parameters related to MW polymerisation (especially power, time and length of polymerisation) would be very interesting to study for its possible effect on the properties of the MIPs as it would potentially give indication of optimal conditions for using MWI.

The study presented in this paper focuses on understanding the effect of different experimental parameters on the physical and chemical properties of a MIP prepared through microwave irradiation, with an aim to identifying MWI conditions that favour MIP synthesis. To do so, a series of MIPs specific for caffeine have been prepared by MWI, based on the 2010 study by Turner.[13] Caffeine has been selected due to its stability (potential degradation of template would add another unwanted factor into the equation) and that it is a well understood system. Factors studied are polymerisation heating rate, length of polymerisation and polymerisation temperature. A series of the NIPs (non-imprinted polymers) have also been prepared for every MIP created as negative controls, and both sets compared to those prepared by traditional oven and UV polymerisations as positive controls for the MW polymers under study. The obtained polymers have been characterised by different analytical techniques (such as, BET, DSC, TGA, SEM, HPLC) to understand their physical properties and template recognition performance. As an aside a separate short study on solvents and cross-linkers has been performed with the aim to explore the validity of MWI for general use in MIP synthesis.

Results and Discussion

Synthesis

For this work focused on a MIP specific for caffeine based on the Turner study. [13] A standard "recipe" of 1 : 4 : 12 template : monomer : crosslinker (caffeine : methacrylic acid : EGDMA) in acetonitrile with AIBN as the initiator was used. This was selected as it represents a bulk polymerisation system commonly used in the MIP community, so it would easily purpose as a model. Synthesis was carried out in the same vessel type for all reactions ensuring that prepared materials could be compared across methods.

Initially the temperature required for polymerisation within the microwave was studied. AIBN is known to break down at ~55 °C in thermal reactions (and far lower under UV). We selected a power of 5 W for this as we wanted to include this low power in our study range. Under 5 W irradiation, no polymerisation was observed at the temperatures of up to 50 °C, neither exothermic behaviour (from auto-acceleration) nor a successful polymerisation was observed. For the temperatures of and above 60 °C, the observed exothermic nature of the reaction was indicative of a successful polymerisation, therefore we selected 60 °C, as our cut-off temperature. This also is in agreement with the prior study and is a temperature that we know will decompose AIBN in an oven, so is comparative – 60 °C is a common standard temperature used for thermal polymerisations.[5] It was noted that setting the temperature higher (at 75 °C or 90 °C) did lead to faster kinetics for the 5 W curve (supporting information), but this was expected as energy put into the system will drive the polymerisation reaction. Given that we wanted to explore the effect of power the minimal temperature where reaction was observed was selected.

Next, a brief study on length of polymerisation time was performed (data not shown). For comparative means the system required a minimum of fifteen minutes (900 seconds) to equilibrate back to 60 °C at the lowest power studied. Leaving the reaction vessel in the microwave for longer had no negligible effect on the polymer materials as the reaction had clearly completed. Likewise, removing it sooner meant for some polymers the reaction had not fully completed.

Figure 1 (Top) shows the temperature profiles of the polymerisation reactions at different powers. Several trends are observed in this. Firstly, and most obvious, is the maximum temperature reached in each reaction. The centre graph on Figure 1 shows a good correlation between the two suggesting that the power applied has a significant effect on the kinetics of the reaction.

The second trend is the rate of temperature increase after the system has reached 60 °C, where no further irradiation is applied. There is a clear correlation between the applied power and the rate of auto-initiation (Bottom graph – Figure 1), suggesting that there is an effect on the rate of initiator decomposition, matching the findings of Ergan. [27]

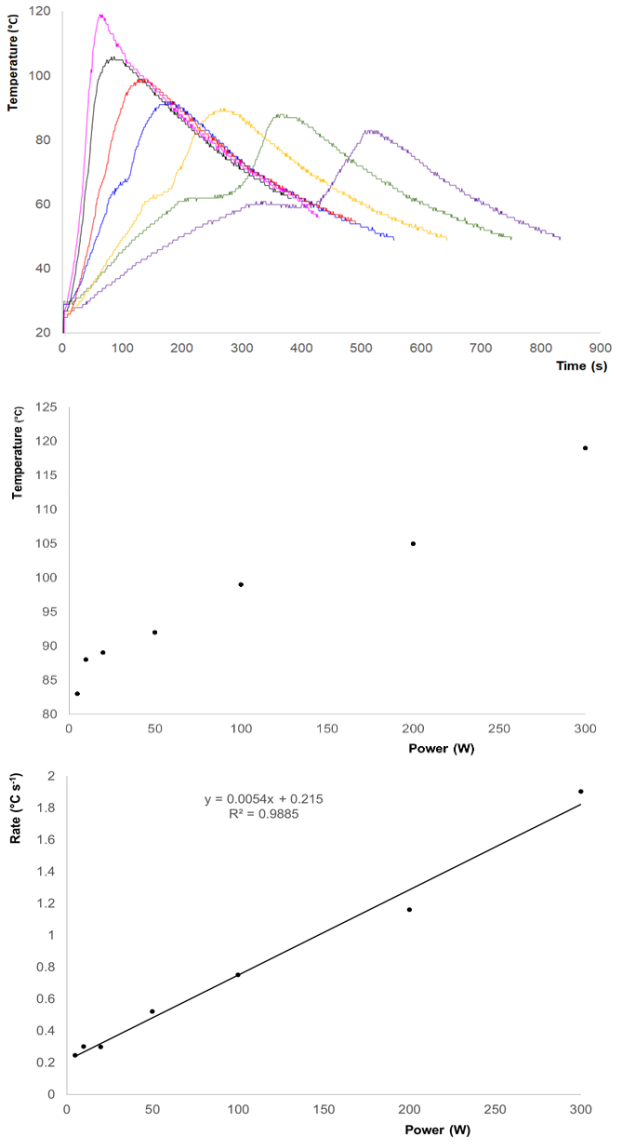

Figure 1: *Top:* Temperature curves during synthesis, measured via in-situ IR probe. In order left to right. 300W – Magenta. 200W – Black. 100W – Red. 50W – Blue. 20W – Yellow. 10W – Green. 5W – Purple. *Centre:* Maximum Temperature reached vs irradiation power (W). Microwave irradiation applied at stated power until 60 °C then reduced to 0W. *Bottom:* Rate of self-generating temperature rise after irradiation cut-off vs irradiation power (W). Calculated from observed point of auto-acceleration start.

ARTICLE

Table 1: Representative surface area and total monomer conversion for MWI polymers. Note that tested materials were the monoliths and not the residue. SD's are result of triplicate experiments.

MW Power (W)	Surface Area ($m^2 g^{-1}$)	Average Pore Radii (Å)	Average Pore Volume ($cm^3 g^{-1}$)	Glass Transition Temperature (°C)	Total Monomer Conversion (%)
5	206 +/- 3	52.5 +/- 0.4	0.54 +/- 0.1	78.0 +/- 1.2	98.57 +/- 0.01
50	192 +/-4	52.1 +/- 0.3	0.51 +/- 0.1	76.5 +/- 1.3	99.60 +/-0.02
150	186 +/- 2	51.9 =/- 0.5	0.42 +/- 0.1	74.1 +/- 1.4	99.75 +/- 0.01
300	151 +/- 2	52.9 +/- 0.2	0.42 +/- 0.1	62.5 +/- 0.3	99.98 +/- 0.01

Thirdly, after irradiation cut-off there is an intermediate period where the reaction slows before auto-acceleration becomes prominent. At the highest power (300 W) there is no clear reduction in rate after the cut off, but it becomes noticeable as power decreases (a very slight change at 200W, becoming more evident through 100 W to 20 W). At 10 W and 5 W there is a clear period where the reaction temperature holds at or near the cut-off temperature before energy generated by the reaction takes over and generates a renewed increase. This period is longer for 5W than 10W following the trend, however the time spent at 60 °C is roughly the same for both before an observed slight drop in temperature in the 5W sample before the exothermic auto-acceleration reaction is observed.

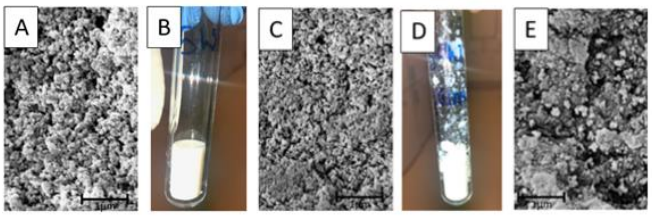

Figure 2: Observed materials. A: Representative SEM micrograph of 5W polymer monolith. 30,000 x magnification. B: Photograph of reaction vessel showing 5W monolith. C: Representative SEM micrograph of 50W polymer monolith (lower material). 30,000 x magnification. D: Photograph of reaction vessel showing 50W monolith with sprayed residue (collected form upper portion of the tube). E: Representative SEM micrograph of 50W polymer residue. 30,000 x magnification.

If we consider this as just a thermal heating effect, we would work on the principle that AIBN does not decompose until 55 °C then it would be expected that there would not be such a significant difference as the reaction would not start until it reached this point, however these results clearly show an effect of the microwave heating on the degradation of the initiator. This is in agreement with Ergan who noted known that the decomposition kinetics of AIBN (*k* increases) alters at increasing microwave power. Given that the *k* of decomposition is a clear driver of a free-radical polymer reaction this is not surprising, but it is interesting that there is such a clear trend between power and reaction rates, both below the cut off and above.

Visual observations of the resultant polymer were striking (Figure 2). The reactions shown in Figure 1 were allowed to run for 15 minutes before removal from the reactor. At lower powers (=/< 20W) the resultant polymer monolith was a clean even block at the base of the vial with all material appearing homogenous (Figure 2B). These resembled the same mixture polymerised under UV or thermally in the oven. However above 50W there was a distinct heterogeneity in the polymer (Figure 2D). A smaller monolith was observed within the bottom of the tube, but a crumbly less robust material would be found sprayed throughout the vessel. This is expected as at lower powers, the porogen has not been boiled away as fast allowing it to stay within the material. The boiling point of the porogen, in this case acetonitrile, is 82 °C means that it is likely to have evaporated quicker at higher powers with bubbling through boiling forcing some material away from the monolith at the bottom of the tube, where the microwaves are focussed. This residue was clearly reacted polymer but unlike the monolith which was bright white, this residue had a duller white-grey colour suggesting a very different morphology to the central monolith. Potentially as this residue is out of the line of the focused microwave irradiation it could be polymerised more through thermal effects than microwave. SEM of the materials confirmed a significant difference between polymer materials (Figure 2). At lower power (Figure 2a) the material appears to be more porous when compared to higher powers (Figure 2c). At higher powers the material visually appears less porous. This is supported by the BET surface area data shown in Table 1, where polymers made at lower power, with a slower rate of growth and lower overall temperatures have a higher surface area. The "spray" residue from higher powers has a very different morphology (Figure 2e) suggesting that it has not formed in the same conditions.

Interestingly, while the monomer and template boil well outside of the temperatures measured (161 °C and 178 °C respectively) the cross-linker EGDMA boils at 98 °C suggesting that it also could be adversely subject to the rapid temperature increases observed at higher concentrations. The reaction vessel temperature quickly exceeds the boiling point of EGDMA for higher heating rates (MW power) indicating the crosslinker may have reacted almost

exclusively in the gaseous state whilst the remaining reaction mixture was likely still in solution. In effect the gaseous expansion of the crosslinker will make it act as an additional blowing agent – and is likely responsible for the sprayed residue (Fig 2D). The total monomer conversion amounts (Table 1) are inversely proportional to power. While conversion is high for all of these (>98%) there is a measurable difference between low and high powers

Physical Properties

The average pore radii of the MWI MIPs was found to be much similar (Table 1) throughout the range of MW power they were polymerised with (from 5 W to 300 W). In all cases, the radii of the pores did not vary considerably. The results observed here are comparable to those observed in prior work[13] which shows the pore breakdown of a similar microwave polymer. Having similar sized pores in all the MIPs with different surface area and different pore volumes also suggested that the depth and the number of the pores could vary in order to compensate for the available surface and volume of the polymer matrix. This could be highly dependent on the rate of heating, intrusion pattern of porogen and the degree of cross-linking of the polymer. The pore volumes of (Table 1) were found to vary depending on the heating rates (MW powers) with which they were polymerised. Total pore volume of the MW MIPs decreased slightly when the MW power was increased. This suggested that slower heating rates (lower MW powers) produced MIPs with larger pore volumes. No such study has been reported investigating such behaviour of MW heating parameters in the context of morphology of the resulting MW MIPs though prior work by Turner [13] showed this difference between traditional (oven heated) and microwave materials. But this behaviour could be understood by studying the polymerisation kinetics.

In a traditional thermal initiation, the rise in temperature would be much slower than in the microwave. Hence, porogen would get to intrude more and deeper between the growing polymeric chains before extensive cross-links could be formed. As a result, they might show higher pore volumes. In this study, MW polymerisations carried out with slower heating produced MIPs with higher degree of cross-linking and higher pore volumes too. From this, a hypothesis could be that unlike inconsistent oven heating, the constant pulsatile MW heating might enforce the porogen to enter the growing nuclei repeatedly in spite of having sufficient cross-linking. More porogen intrusion could then result into higher pore volumes at the same time having higher degree of cross-linking.

DSC analysis is a routinely used to characterise cross-linked polymers for their glass transition temperatures (T_g) which is an indicative of their degree of cross-linking. The thermograms obtained were further analysed and their T_g values obtained. The T_g values were inversely proportional to the MWI powers (and therefore reaction rates) The highest T_g was obtained with the slowest heating rate (5 W) and the lowest T_g was obtained with the highest heating rate (300 W) (Table 1). As the slower heating rates (5W) provides a larger window for the polymerisation reaction to incorporate the EGDMA crosslinker into the MIP before exceeding its boiling temperature a greater degree of crosslinking could be expected.

Analysis of thermal degradation (measured via TGA) indicates further complications and potential heterogeneity within the samples (Figure 3). All the samples show a mass loss of approximately 2% at 50 °C, due to solvent loss or atmospheric moisture loss. Sample 5W shows the largest loss and sample 200W the lowest. Sample 5W appears to have the lowest mass loss during the main decomposition step, 299 °C, with a 90.5% loss. The other samples have a higher mass loss during this decomposition, 329-338 °C, with an average mass loss of 92.38%. Sample 5W shows total decomposition by 500 °C whilst the other samples still have a residual mass of ~0.15% at 500 °C. The comparative literature indicates PMMA will begin decomposing rapidly when heated above 220 °C often via a first-order unzipping or end-thermal scission to produce monomer.[28] Crosslinking can significantly alter thermal stability, shifting the degradation onset temperature up to above 300 °C, but can then both increase or decrease with varying levels of crosslinker.[29]

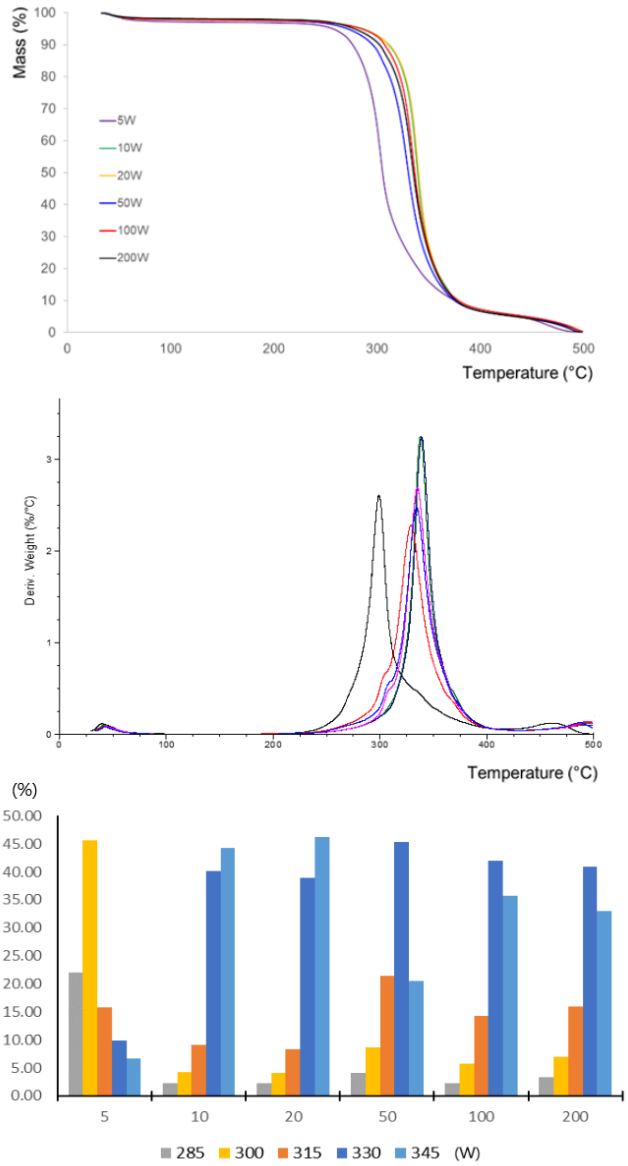

Figure 3: Top: Thermogravimetric Analysis (TGA) mass loss profiles for polymers synthesised under a range of different irradiation powers. 200W – Black. 100W – Red. 50W – Blue. 20W – Yellow. 10W – Green. 5W – Purple. **Middle:** Derivative of mass loss with temperature. 5W -Black, 10 W – Green, 20 W – Dark Blue, 50 W – Red, 100 W – Pink, 200 W – Light Blue. **Bottom:** $\%T_{TGA}$ (area deconvoluted peak) for 15 °C temperature ranges across second observed degradation step.

In this instance the sample prepared with a 5W heating rate was clearly distinct to the other MIPs with the main decomposition event occurring at 300 °C as opposed to 330-340 °C, in line with literature data that indicated higher levels of EGDMA crosslinking reduces thermal stability. [29] However comparison of the derivative mass loss (Figure 3B) shows that all materials had a broad decomposition range occurring over a 70 °C area. All samples show one main decomposition and the onset temperature is the same for all at 220 °C. The temperature at which the rate of decomposition is greatest does vary between samples. For sample 5W it is 299 °C whist the others fall between 328 and 338 °C. Sample 5W shows a shoulder on the right-hand side of the decomposition peak at 337 °C. Samples 50, 100 and 200 °C show a shoulder on the left-hand side of the decomposition at ~300 °C. The third decomposition is at 460°C for sample 5W whilst it is still ongoing at 500 °C for the other samples.

For samples with the highest heating rate (200 – 50 W) the derivative weight loss shows an increasing shoulder at 300 °C that is absent in the medium heating rates (10 – 20 W). This was confirmed via a deconvolution of the derivative mass loss into five thermal events, and the $\%T_{TGA}$ of these 15 °C intervals shows the changing properties of the analysed samples (Fig 3C). The stark contrast between the 5W and the other samples can now be quantified as over the studied temperature range 68 % of this second decomposition comes from the 285 / 300 °C components, with only 32% arising from higher temperature ranges. With other samples this low temperature % contribution changes to 7, 6, 12, 8 and 10% respectively – indicating that the 300 °C shoulder does not change significantly for the other samples. What does vary between the other samples is the relative contribution at 315, 330 and 345 °C centred distributions – and so whilst the 10 and 20 W samples show a narrow derivative to the mass loss (occurring between the 330 – 345 deconvoluted peaks) this broadens at higher wattage as the 315 °C contribution increases significantly.

Although the MIP materials are a mixture of several monomers PMMA-crosslinked with EGDMA are the main components that will dominate thermal instability. This can be directly correlated by whether the reaction vessel immediately auto-initiated and the temperature rose above the boiling point of EGDMA or whether the reaction has time to incorporate the crosslinker at 60 °C before further temperature rises occurred (and the spraying of residue observed in Fig 2D). The rising shoulder (300 °C) at the higher heating rates can be linked to a growing EGDMA fraction (that would likely have reacted in the gaseous phase) whilst the decomposition at 330-340 °C arises from less densely crosslinked material. Although the MIP material is a mixture of several monomers MAA and EGDMA are the main components and so will dominate the thermal decomposition profile.

These results overall suggest that it might be beneficial to use slower MW heating to produce polymers with larger surface area, higher porosity and higher (homogenous) levels of cross-linking at the same time.

Rebinding Performance

Analysis of the polymers for rebinding was performed with a simplistic SPE system. Differing concentrations of caffeine solution (0.2 mM – 0.7mM) were filtered across the polymers. Using HPLC as for analysis, bound template was measured. amount of caffeine bound to the MIP was then calculated from HPLC results and plotted against the total amount of caffeine introduced to the polymers in SPE. For this study we are not interested in achieving 100% binding as we would have to take into account other factors such as SPE bed depth, monomer selection, flow rate etc. Here we are looking to compare the performance of the synthesised polymers against each other. From Figure 4A we can observe that performance is almost identical for 5 W and 50 W polymers with a slight drop off at 150 W and a significant drop at 300 W. For all polymers there is a capacity affect with more template bound percentage wise at lower concentrations than at higher but this also drops off in the higher power polymers.

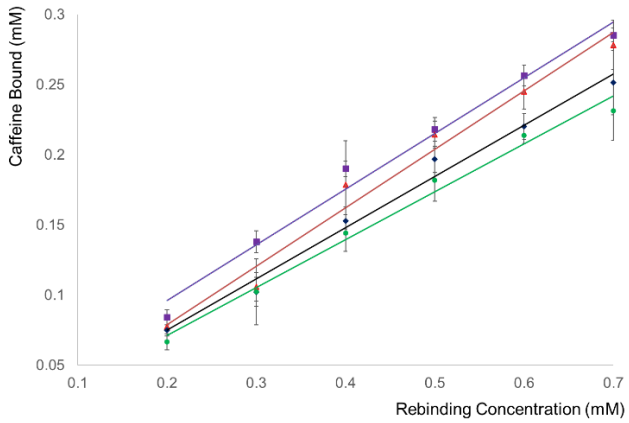

Figure 4: Rebinding of caffeine at different concentrations for polymers made at different powers. Purple square with purple line = 5 W. Red triangle with red line = 50 W. Black diamond with black line = 150 W. Green circle with green line = 300 W. Samples measured in triplicate. Standard deviations shown were derived from the triplicate measurements of each sample.

Similar caffeine binding measurements were carried out on the parallel set of the NIPs (see supporting information) and the imprinting factors (IF) were calculated as *"amount bound to MIP / amount bound to NIP"*. The resultant data highlighted that the 5W MIP gave an average IF of approximately 1.5, while this was reduced to ~1 for the 300W material (see supporting information for table). It should be noted that IF can be used as a guide to the validity of an imprint but it is not a definitive figure, as it doesn't take into account differences in the physical properties of the materials (surface area, porosity etc.) It has also been noted that higher values of IF would be regarded as an indicative of the non-selective template binding of the NIPs than improved imprinting efficiency of the MIPs.[27] These data show, in correlation to the rebinding the higher power polymers performed worse while lower powers were comparable. This indicated the presence of an equivalence of both the selective and non-selective binding sites present within the MIPs, with the percentages rebound being higher at lower concentrations suggesting that high affinity pockets fill up first. Either way these figures are comparable to existing literature. [13]

Rebinding of further lower template concentrations could be useful in preparing a Scatchard plot for better understanding of the selectivity of the binding sites; however, the concentrations below 0.05 mM were not detectable (below LOD) using the HPLC instrumentation available. That the 300 W polymer did not exhibit imprinting (IF ~1) suggests that as higher reaction rates are the chance of high-quality imprinting is lowered. It is known that the formation of imprints is under thermodynamic control and using

such a high amount of energy in synthesis probably disrupts this formation.[30]

Also, given the observed "blow" on higher power polymers (> 50 W), that we hypothesise is caused by boiling of EGDMA, we also have to factor in the effect of the cross-linker on MIP performance. It is accepted that the cross-linker to monomer ratio is key to an effective imprint due to effects of binding pocket composition and morphology. Changes here will have a significant effect.[31,32]

Selectivity studies (using theophylline) were performed for the range of polymers (supporting information). All polymers except the 300 W one exhibited selectively towards caffeine in a comparable fashion to data observed in prior work.[27] The 5 W polymer exhibited slightly higher selectivity, and the 300 W polymer showed no selectivity between the two compounds correlating with the suggested lack of imprinting observed. This combined with the data in Figure 4 and the suggested imprinting effect hinted at by the IF's suggest that a lower power initiation is beneficial over a "hard" high power exposure.

Alternate component selection

For this to be a practical alternative to using thermal or UV polymerisation different components need to be considered. MIPs are synthesised with a vast range of components as functional monomers, cross-linker, initiator and porogen. We performed a simple short study using the same component "recipe" as above, replacing porogen (acetonitrile with chloroform) and/or the cross-linker EGDMA with either divinylbenzene (DVB) or trimethylolpropane trimethacrylate (TRIM). These were selected as they are common components which feature often in the literature. The microwave system was set at 10 W for 15 minutes with a standard cut-off at 60 °C. The purpose here was not to test these materials for their imprinting properties but to explore the potential of using alternative components during MWI.

Table 2: Relevant physical properties of common solvents

Solvent	*Acetonitrile*	*Chloroform*
Permanent dipole (D)	3.92	1.15
Dielectric constant (ε)	37.5	4.81
Tan ∂	0.062	0.091
Boiling point (°C)	82.0	61.0

Standard microwave ovens utilise the non-ionising, electromagnetic radiation microwaves to penetrate the sample and vibrate the molecules within the sample. Efficient heating of molecules by microwave dielectric heating and is directly dependant on the materials ability to absorb microwave energy and convert it into heat energy. Microwaves induce an electromagnetic field causing heating by two main mechanisms: dipolar polarisation and ionic conduction. Irradiation of the sample causes the dipoles or ions to rotate as to align to the applied electric field as it oscillates. This results in lost energy in the form of heat through friction and dielectric loss.[33]

The ability of the matrix to heat via dielectric effects is attributable to the samples ability to form this dipole moment. If a sample cannot form a dipole moment or the dipole does not have enough time to align to the field no heating will occur. This can be expressed as a sample's dissipation factor (tan∂). Solvents can be classified as high (tan∂ > 0.5), medium (tan∂ = 0.1-0.5) and low microwave absorbing (tan∂ < 0.1).[33] The choice of solvent is very important in synthesis as it helps governs the heating rate – something that will be critically important in the thermodynamic control of imprinting and the degradation of the initiator.

Acetonitrile is especially useful as a solvent for the synthesis of polymers via microwave. Studies have emphasised the application of acetonitrile for organic synthesis,[34] while chloroform is used far less. However, in the field of imprinting both are commonly used, hence it is important to see how they differ. Table 2 summarises the physical properties of the solvents. A high dipole value correlates to the system's ability to convert microwave energy into heat energy suggesting that acetonitrile should be more efficient.

Changes in solvent

Four polymers (two pairs) were synthesised to the same ratios as above. The power was set at 10 W for 15 minutes with a cut-off temperature at 60 °C. The first pair had EGDMA as cross-linker and were made in either acetonitrile or chloroform. The second pair substituted TRIM as the cross-linker and were made in the same solvents. The top graph in Figure 5 shows the polymerisation kinetics through heating of the four polymers. The polymers made in chloroform reached the cut-off temperatures significantly faster than those made in acetonitrile and the final temperatures reached were comparatively higher, which could be explained by an increase in pressure as the solvent goes through gaseous expansion.

Visual analysis of the polymers (Figure 6) shows that both polymers made in chloroform appeared denser than their respective acetonitrile counterpart, with smaller nodules (agglomerated particles), leading to higher porosity on the macroscale. This correlates with the results in Figure 2, where a polymer made at a faster rate also exhibits these traits. This suggests that in chloroform the rate of initiator breakdown is higher, leading to more nucleation sites and smaller nodules. Combined with the lower boiling point, affecting its activity as a porogen, the resultant polymer is denser. This suggests that the acetonitrile was a more successful porogen in terms of enabling consistent polymerisation to occur. Porosity is important to enable effective flow through the material.

Despite the fact the polymerisation in the chloroform prepared samples will almost exclusively be occurring with the solvent having transitioned to the gaseous phase, the effect of switching solvent on the product T_g offers no clear evidence that a change in crosslink density has occurred (see supporting information). When analysed by TGA, similarly to previous samples the majority of the thermal degradation occurred over the second degradation step and that some samples had not fully degraded by 500 ^{o}C.

The second degradation showed increased variance compared to samples prepared at varying microwave power – and as before were fitted to gaussian peaks using the same equation as before. Comparison of the low power components of the fitted peaks (285 and 300 ^{o}C centred peaks) represented 71, 31, 35 and 19% of the decay across the series. With the exception of the EGDMA – MeCN sample the 315^{o}C centred peak dominated with 29, 68, 64 and 80% contribution to the total decay indicating three of the samples represent narrow decomposition profiles.

Further direct comparison of the mass loss between the samples show there is a generalised increase in thermal stability as the decays are generally shifted to a higher temperature (supporting information). This supports the conclusion that the polymers are less densely crosslinked.

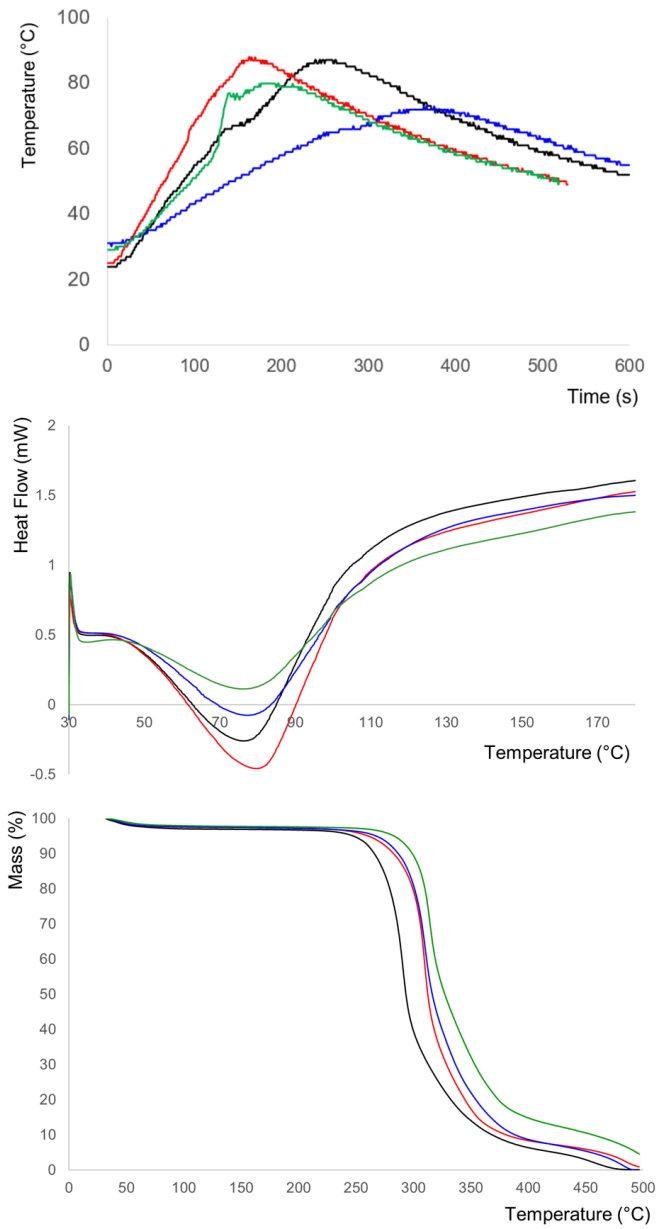

Figure 5: Heating profiles (**top**), representative DSC (**centre**) and TGA (**bottom**) traces for polymers synthesised with differing solvents and cross-linkers Black: Acetonitrile – EGDMA. Red: Chloroform – EGDMA. Blue: Acetonitrile – TRIM. Green: Chloroform – TRIM**.**

Changes in cross-linker

Three cross linkers are commonly used in traditional bulk imprinting. EGDMA, TRIM and divinylbenzene (DVB), with popularity in that order. As described in 3.4.1, polymers, in both chloroform and acetonitrile, were synthesised and tested. Under the same conditions attempts to polymerise the same mixture with DVB as the cross-linker failed in chloroform, while in acetonitrile, after the 15 minutes the reaction mixture had formed a milky solution suggesting that polymerisation was occurring but at a significantly slower rate. SEM of the material (data not shown) supported this with small nodules formed.

This pattern was also observed in test materials where the MAA and template were removed. This suggests that DVB will polymerise but will require longer period or increased energy. It is an interesting finding, as the heating profile data in Figure 5 suggests that EGDMA and TRIM bearing polymers polymerise more rapidly in chloroform than in acetonitrile, but DVB doesn't react. This suggests that there may be an interaction between the solvent and monomer which affects its susceptibility to polymerisation.

DVB has been considered in the manufacture of microwave transparent materials[35,36] while another study shows that much higher temperatures (120 °C) were required to obtain polymerisation [37] – temperatures that would be unsuitable for MIP synthesis due to thermodynamic requirements.

From the heating profiles in Figure 5 it is clear that TRIM has a slower reaction rate than EGDMA, with this observed in both solvents. The boiling point of TRIM however is 422 °C, far in excess of any temperature recorded in the vessels, and so unlike EGDMA it is unlikely to enter the gaseous state.

Analysis of the samples by DSC and TGA show negligible differences in glass transition temperature between the two TRIM samples with potential higher thermal stability for the chloroform solvent material (supporting information).

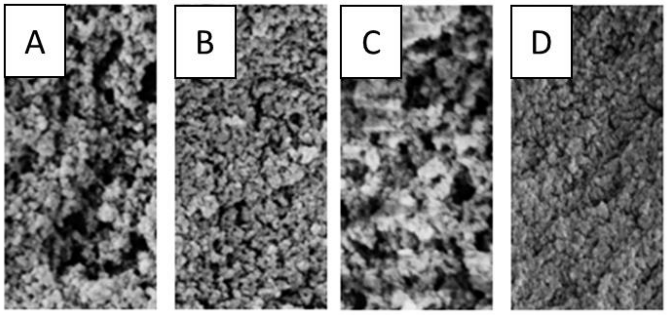

Figure 6: Representative SEM micrographs of synthesised polymers. 30000x magnification**. A:** Acetonitrile – EGDMA. **B:** Chloroform – EGDMA. **C:** Acetonitrile – TRIM. **D:** Chloroform – TRIM.

Experimental

Materials

Methacrylic acid (MAA), ethylene glycol dimethacrylate (EGDMA), acetonitrile, 2,2'- azobis (2-methylpropionitrile) (AIBN), trimethylolpropanetrimethacrylate (TRIM), divinylbenzene (DVB), caffeine were purchased from Sigma-Aldrich (UK).

Toluene, chloroform, methanol (MeOH), glacial acetic acid, dimethylformamide (DMF) were of HPLC grade and were purchased from Fisher Scientific (Loughborough, UK). Double distilled ultrapure water (Millipore, Livingston, UK) was used for analysis.

The solid phase extraction (SPE) tubes (Supelco, 1ml) were purchased empty from Sigma-Aldrich (Gillingham, UK) along with frits (20 µm). The Pyrex glass-tubes)10 mL) used for polymerisation were purchased from Discover (Buckingham, UK). Specialist materials for TGA, DSC and BET (sample holders) were purchased from Fisher Scientific (Loughborough, UK).

Polymer Synthesis

Polymer monoliths were prepared by imprinting caffeine as a similar protocol was used as reported by Turner. [13] 97 mg of caffeine (0.5 mmol) was dissolved in 2 mL acetonitrile in a 10 mL test-tube. 0.175 ml of MAA (2 mmol) and 1.248 ml EGDMA (6 mmol) were added to the mixture in the test-tube, giving a ratio of 1:4:12 Template/Monomer/Cross-linker. This mixture was sonicated for 5 minutes until all components were dissolved completely. AIBN (15 mg, 0.09 mmol) was then added to the reaction mixture in the test-tube followed by degassing with nitrogen sparge for 10 minutes. Where an alternative solvent or cross-linker was used to explore the validity of using MWI for making these polymers, the molar ratios were kept the same as above.

The test-tube was sealed using a specialist cap and placed in a 2.45 GHz CEM Discover Benchmate MW reactor (CEM Corp., UK) under the different experimental conditions that were explored These conditions are described in the results section. Specified powers were used to heat the polymerisation mixture to attain the desired temperature. When the set polymerisation temperature was attained, the MW system turned off (0 W) and no further irradiation was applied. Any further change in the polymerisation temperature beyond this would not be due to MWI but due to the exothermic energy generated as a result of the free radical reaction.

Polymerisation temperature was recorded throughout the polymerisation reaction through Synergy™ interface via an *in-situ* infra-red temperature probe.

After the reaction has finished the tubes containing the polymeric monolith were removed from the reactor and allowed to cool to room temperature. The monolith was then wet ground using methanol and sieved (Endecotts, UK) to obtain a particle size range between 45 µm and 63 µm. The desired particle size fraction was subjected to Soxhlet extraction in acidified methanol (10 % acetic acid) for 24 hours to remove template and unreacted materials. This was repeated twice and wash solutions tested until no trace of caffeine or other reactants were detectable (by HPLC). Polymers were then dried and stored at the room temperature in sealed vials.

Control polymers were also prepared by oven and UV polymerisation. Oven polymerisation was carried in a similar sealed Pyrex test-tube using a forced air circulation oven (Memmert, Germany) at different temperatures (60 ˚C to 90 ˚C) for different time durations (from 4 hours to 24 hours).

The UV polymers were prepared by using exactly same polymer *recipe* using a shortwave (CL-1000, 245nm) UV cross linker bench top reactor (UVP, CA, USA) with exposure delivery of x100 µJoule cm^2 by varying polymerisation time and temperature as summarised in the following tables below. UV polymerisation was carried at 0 ˚C and 20 ˚C for different times (from 4 hours to 24 hours). As this is a comparison of performance of the imprinted materials, non-imprinted polymers (NIPs) were not considered.

Polymerisation Kinetics

Polymerisation temperature profiles were recorded per second for the MW polymers via in-situ IR temperature probe inserted into the MW reactor (CEM Benchmate, CEM Corp UK) and were calculated into heating rates (°C $minute^{-1}$) where required.

Total Monomer Conversion

Total monomer conversion was calculated for the polymers prepared by MW reactor. UV spectrophotometry was used to calculate the total monomer conversion into the polymer under different polymerisation conditions. Polymer monoliths obtained from the MW reactor were ground dry with the aid of mortar and pestle for 5 minutes. The powered polymer was filled into the cellulose extraction thimbles for Soxhlet extraction and was subjected to Soxhlet extraction in analytical grade methanol for 24 hours. Polymer fines were allowed to sediment and aliquots of 2 ml of extracts were taken for each sample. A six-point calibration curve of the monomer mixture (0.095 mM to 2.95 mM) was produced in methanol by the UV spectrophotometric analysis of the mixture at 220 nm in triplicate. Samples were filtered, dried down, re-suspended into 1mL methanol. These methanolic extracts of polymer washes were then analysed for their absorbance by UV spectrophotometry (Jasco, UK) and the amounts of the monomers in the extracts were calculated from the calibration curve produced earlier. The amount of the monomers (mM) leached out in the Soxhlet washings was then subtracted from the total amount of the monomers used in the polymerisation to calculate the amount of the monomers converted to the polymer. The monomer conversion amounts were then calculated as the % of the original mixture for all the MIPs and the NIPs prepared through the range of microwave powers, temperatures and the lengths of the polymerisation.

Differential Scanning Calorimetry (DSC)

To carry out the analysis, approximately 2 mg of sample was placed in a TA standard aluminium DSC pan and press sealed with a standard aluminium lid. Analysis was carried out on a TA instrument Q2000 with data processing using TA Universal Analysis software. The sample was run against an empty reference pan from 30 °C to 200 °C at a rate of 10 °C/minute, held isothermally fr three minutes before cooling to 30 °C at a rate of 50 °C/minute.

Thermogravimetric Analysis (TGA)

Thermogravimetric analysis was used to analyse polymer samples for their degree of cross-linking and carried out on a TA instrument Q5000. Approximately 2 mg of each sample was placed into a platinum high temperature TGA pan. The pan had been cleaned using a butane blow torch and tared using the automated tare function. The samples were heated from ambient to 500 °C at a rate of 10 °C/min. The mass loss percentage was calculated via the following equation

$$\%\ \boldsymbol{mass\ loss} = \frac{\boldsymbol{Initial\ mass - Final\ mass}}{\boldsymbol{Initial\ mass}}\mathbf{100}\%$$

The distribution of mass loss via thermal decomposition (from 280 and 350 °C) was analysed by fitting the derivative mass loss to five gaussian distributions, each generated using the equation:

$$\boldsymbol{Y = exp}\left(-\frac{\frac{(\boldsymbol{X-\mu})^{\mathbf{2}}}{\mathbf{2}\times\boldsymbol{\sigma}^{\mathbf{2}}}}{\boldsymbol{\sigma}\times(\mathbf{2}\times\boldsymbol{\pi}^{\mathbf{0.5}})}\right)$$

where µ was 285, 300, 315, 330 and 345 °C respectively and σ was fixed as 2. A deconvolution extracting these five peaks with varying relative areas (I_μ) was carried out. The relative % contribution to

thermal degradation at each of these temperature $\%T_{TGA}$ is then quoted within the manuscript for each specified μ.

$$\%T_{TGA} = \frac{I_{\mu}}{\sum I} 100\%$$

Porosimetry

Porosimeter and surface area analyser Nova 1000e (Quantachrome, UK) was used for this analysis. To carry out the analysis, 20 – 30 mg of sample was first degassed at 110 °C under vacuum for 1 - 2 hours to remove any adsorbed solvent. Determinations of specific surface area were performed using an ASAP 2000 instrument (Micrometrics) based on the nitrogen multi-point BET method (maximum experimental error < 1 %). This was repeated in triplicate using different aliquots of the same polymer sample.

Water permeability measurements were performed in a UF cell (*d* = 25 mm, model 8050, Amicon Corp.) using different hydrostatic pressures as driving force. The adsorption isotherm of this degassed sample was then measured using nitrogen as the absorbate at a temperature of 77 K covering the partial pressure (P/P_0) range of 0.05 to 0.35.

The specific surface area of each sample was automatically calculated from the slope and the intercept using the linearised BET equation.

$$\frac{1}{[W(\frac{P_0}{P}-1)]} = \frac{C-1}{W_m C} * \frac{P}{P_0} + \frac{1}{W_m C}$$

where,

P = partial vapour pressure (Pa) of the adsorbate gas;

P_0 = saturated pressure (Pa) of adsorbate gas;

W = volume of gas (ml) adsorbed at standard temperature (273 K) and pressure ($1X10^5$ Pa) (STP);

W_m = volume of gas (ml) adsorbed at STP to produce a monolayer on the surface of the sample;

C = dimensionless constant related to the enthalpy of adsorption of the gas on the sample surface.

The pore size distribution and volume was calculated using a density functional theory (DFT) based approach using Nova 1000e Surface Area (by using Quantachrome™ Novawin2 software).

Scanning Electron Microscopy

The ground polymer samples were sprinkled onto the carbon sticker and then coated with gold using POLARON sputter coater at 2.0 kV coating voltage for 2 minutes to give the coating thickness of around 20 - 25 nm. The samples were handled by the specimen holder and viewed under Zeiss Supra 55VP FEG SEM at 250X and 5KX magnification.

Solid Phase Extraction

Solid phase extraction (SPE) was used to analyse the template rebinding performance of the polymers. Each polymer was packed as 100 mg aliquots in triplicate into 1 ml solid phase extraction cartridges (Supelco Ltd, UK). The cartridges were then rinsed with methanol and acetone to ensure even packing and then dried under vacuum. Rebinding solutions of caffeine were prepared in the range of 0.05- 3 mM using HPLC grade acetonitrile (Chromasolv, Sigma-Aldrich, UK). The solutions were passed through the SPE cartridges using a Supelco vacuum manifold connected to a vacuum pump. The flow rates were maintained constant for maintaining 1 mL min^{-1} for the homogeneity of the binding kinetics. The SPE protocol was followed as described in the steps below.

The cartridges were conditioned by using 1 mL HPLC grade acetonitrile. Then 1 mL of the rebinding solution was passed through each cartridge and collected in 1 mL HPLC vials for further quantification. After passing through the rebinding solution, each cartridge was washed thoroughly with 5 aliquots of HPLC grade methanol followed by drying with 1 mL HPLC grade acetone to remove previously bound caffeine to its imprinted polymer. Cartridges were then dried under vacuum for about 15 minutes before introducing another 1 mL aliquot of the caffeine rebinding solution. And then remaining of the steps were followed as described above. The collected caffeine aliquots were subjected to HPLC analysis.

High Performance Liquid Chromatography (HPLC)

Caffeine rebinding solutions (1 mL) collected through the SPE cartridge was subjected to caffeine quantification by using Agilent 1260 INFINITY LC system equipped with 60 mm DAD detector cell (λ_{max} 270 nm, noise level 0.6 μAU cm^{-1}). The LC based quantification of 10 μL caffeine extract was carried out using the mobile phase water: acetonitrile (50:50) (30 ± 0.05 ˚C, 0.1 mL $minute^{-1}$) through reverse stationary phase (ACE Excel 3 Super 18, 150 x 4.6 mm, EXL–111–1546U). Caffeine calibration curve was prepared in the concentration range of 0.02 mM to 3 mM under identical conditions and was used for the quantification of the unbound caffeine extracts collected from MIP-SPE. The amount of unbound caffeine was then deducted from the total amount of caffeine introduced to the SPE MIP cartridges, to give a bound value. This was plotted against the total amount of caffeine introduced.

Conclusions

The results of this study indicate the advantage of low power rates for maintaining control over the polymerisation process in MIP preparation. They also demonstrate the benefits of reporting peak reaction temperature during the MWI polymerisation process, alongside the physical characteristics of the resultant material, especially when comparing like with like for performance means. Microwave reactors offer the ability to rapidly heat reactants to a target temperature in a uniform manner, however excessive heating rates can trigger rapid further auto-initiation and an exotherm which reduces control of the product.

Detailed analysis of the thermal properties of these materials indicate that the ratio of cross-linker is not directly proportional to the heating rate, and the observed reduction in binding efficiency observed at higher heating rates may partially arise from heterogeneity of the sample composition. The boiling point of both the solvent and all constituent monomers appear to play a critical role in the homogeneity of the product sample. Furthermore, some cross-linking materials appear not to incorporate at all into the product under the tested conditions.

MIPs, while outwardly presenting a simple polymerisation option, often a co-polymer between a single monomer and a cross-linker, have a number of other factors that need to be considered for them to be of practical use. MWI offers an alternative to oven-based thermal polymerisation, but the alternative method of heating can have unintended consequences on product properties. It is not simply a case of forcing a reaction to occur but in order to obtain a successful imprint the requirements are complex. Physical considerations of final material are important (surface area, pore size, rigidity), meaning that control is required for the reaction. It is accepted that the chemical composition of the component mixture is paramount to a successful imprint, but this appears exacerbated in the use of microwaves for MIP synthesis.

The results here are promising in that we are able to control physical properties and link this to performance, but further studies are required for this method to become mainstream in the MIP community. These include the potential for using MWI to support the washing step as well as the synthesis, and exploring the potential using less stable templates under low power conditions. Therefore, in summary, MWI polymerisation of MIP materials offers a potential option for synthetic chemists however the data shown here indicates much further work will need to be carried out to fully control these surprisingly complex systems.

Conflicts of interest

There are no conflicts to declare.

Acknowledgements

NT, CT, and OI would like to thank DMU School of Pharmacy undergraduate project scheme for financial support. CT and OI wish to thank Dr Rachel Armitage and Ms. Leonie Hough for support with SEM analysis.

Notes and references

1 C. Alexander, H. Andersson, L. I. Andersson, R. J. Ansell, N. Kirsch, I. A. Nicholls, J. O'Mahony and M. J. Whitcombe, *Journal of Molecular Recognition,* 2006, **19**, 106-180
2 F. Canfarotta, A. Poma, A. Guerreiro and S. Piletsky, *Nature Protocols,* 2016, **11**, 443.
3 E. Moczko, A. Poma, A. Guerreiro, V. S. Perez de, S. Caygill, F. Canfarotta, M. J. Whitcombe and S. Piletsky, *Nanoscale,* 2013, **5**, 3733-3741
4 C. O. Kappe, *Angewandte Chemie (International Ed. in English),* 2004, **43**, 6250-6284.
5 S. A. Piletsky, E. V. Piletska, K. Karim, K. W. Freebairn, C. H. Legge and A. P. F. Turner, *Macromolecules,* 2002, **35**, 7499-7504
6 I. A. Nicholls, H. S. Andersson, C. Charlton, H. Henschel, B. C. G. Karlsson, J. G. Karlsson, J. O'Mahony, A. M. Rosengren, K. J. Rosengren and S. Wikman, *Biosensors and Bioelectronics,* 2009, **25**, 543-552
7 I. Mijangos, F. Navarro-Villoslada, A. Guerreiro, E. Piletska, I. Chianella, K. Karim, A. Turner and S. Piletsky, *Biosensors & Bioelectronics,* 2006, **22**, 381.
8 J. Jacob, L. H. L. Chia and F. Y. C. Boey, *Journal of Applied Polymer Science,* 1997, **63**, 787-797
9 H. L. Chia, J. Jacob and F. Y. C. Boey, *Journal of Polymer Science Part A: Polymer Chemistry,* 1996, **34**, 2087-2094
10 E. Turiel and A. Martín-Esteban, *Journal of Separation Science,* 2009, **32**, 3278-3284
11 J. Li, S. Li, X. Wei, H. Tao and H. Pan, *Analytical Chemistry,* 2012, **84**, 9951-9955
12 S. Xu, X. Zhang, Y. Sun and D. Yu, *The Analyst,* 2013, **138**, 2982-2987
13 N. W. Turner, C. I. Holdsworth, S. W. Donne, A. McCluskey and M. C. Bowyer, *New Journal of Chemistry,* 2010, **34**, 686
14 N. Saifuddin, C. W. Wong and A. A. N. Yasumira, *E-Journal of Chemistry,* 2009, **6**, 61-70
15 N. Saifuddin, Y. A. A. Nur and S. F. Abdullah, *Asian Journal of Biochemistry,* 2011, **6**, 38-54
16 Y. Zhang, Y. Li, Y. Hu, G. Li and Y. Chen, *Journal of Chromatography A,* 2010, **1217**, 7337-7344
17 Y. Zhang, R. Liu, Y. Hu and G. Li, *Analytical Chemistry,* 2009, **81**, 967-976
18 J. Hou, H. Li, L. Wang, P. Zhang, T. Zhou, H. Ding and L. Ding, *Talanta,* 2016, **146**, 34-40
19 P. Kueseng, M. Nisoa and C. Sontimuang, *Journal of Separation Science,* 2018, **41**, 2783-2789
20 L. J. Schwarz, M. K. Potdar, B. Danylec, R. I. Boysen and M. T. W. Hearn, *Analytical Methods,* 2015, **7**, 150-154
21 Y. Jin, N. Chen, R. Liu, Y. Zhang, L. Bai and J. Chen, *Journal of the Chinese Chemical Society,* 2013, **60**, 1043-1049
22 H. Chen, S. Son, F. Zhang, J. Yan, Y. Li, H. Ding and L. Ding, *Journal of Chromatography B,* 2015, **983-984**, 32-38
23 M. Seifi, M. Hassanpour Moghadam, F. Hadizadeh, S. Ali-Asgari, J. Aboli and S. A. Mohajeri, *International Journal of Pharmaceutics,* 2014, **471**, 37-44
24 M. Schauperl and D. W. Lewis, *The Journal of Physical Chemistry B,* 2015, **119**, 563-571
25 S. A. Piletsky, A. Guerreiro, E. V. Piletska, I. Chianella, K. Karim and A. P. F. Turner, *Macromolecules,* 2004, **37**, 5018-5022
26 S. A. Piletsky, I. Mijangos, A. Guerreiro, E. V. Piletska, I. Chianella, K. Karim and A. P. F. Turner, *Macromolecules,* 2005, **38**, 1410-1414
27 B. T. Ergan and M. Bayramoğlu, *Journal of Industrial and Engineering Chemistry,* 2013, **19**, 299-304
28 W. R. Zeng, S. F. Li and W. K. Chow, *Journal of Fire Science,* 2002, **20**, 401-433
29 Dong Hee Kim, Do Yang Lee, Kang Seok Lee and Soon Ja Choe, *Macromolecular Research,* 2009, **17**, 250-258
30 I. A. Nicholls and H. S. Andersson, in *Techniques and Instrumentation in Analytical Chemistry*, ed. B. Sellergren, Elsevier, 2001, p. 59-70.
31 K. Golker, B. C. G. Karlsson, G. D. Olsson, A. M. Rosengren and I. A. Nicholls, *Macromolecules,* 2013, **46**, 1408-1414
32 G. D. Olsson, B. C. G. Karlsson, E. Schillinger, B. Sellergren and I. A. Nicholls, *Industrial & Engineering Chemistry Research,* 2013, **52**, 13965-13970
33 C. Kappe and D. Dallinger, *Molecular Diversity,* 2009, **13**, 71-193
34 A. P. Jogdand and D. P. L. Kadam, *IOSR Journal of Applied Physics,* 2014, **6**, 14-22
35 X. W. Ye, Y. P. Zhang, L. B. Qu, L. Q. Fan and B. Li, *Chinese Chemical Letters,* 2007, **18**, 1399-1402
36 Y. Chen, J. Mao, Y. Zhu, K. Zhang, G. Wu, J. Wu and H. Zhang, *Journal of Applied Polymer Science,* 2017, **134**, 44865
37 A. Aldalbahi, M. Rahaman and A. El-Faham, *International Journal of Polymer Science,* 2020, **2020**, 1-11